DRTAM: Dual Rank-1 Tensor Attention Module

Hanxing Chi, Baihong Lin*, Jun Hu, Liang Wang

School of Electronics and Communication Engineering
Shenzhen Campus of Sun Yat-sen University, Shenzhen 518170, China

Abstract. Recently, attention mechanisms have been extensively investigated in computer vision, but few of them show excellent performance on both large and mobile networks. This paper proposes Dual Rank-1 Tensor Attention Module (DRTAM), a novel residual-attention-learning-guided attention module for feed-forward convolutional neural networks. Given a 3D feature tensor map, DRTAM firstly generates three 2D feature descriptors along three axes. Then, using three descriptors, DRTAM sequentially infers two rank-1 tensor attention maps, the initial attention map and the complement attention map, combines and multiplied them to the input feature map for adaptive feature refinement(see Fig.1(c)). To generate two attention maps, DRTAM introduces rank-1 tensor attention module (RTAM) and residual descriptors extraction module (RDEM): RTAM divides each 2D feature descriptors into several chunks, and generate three factor vectors of a rank-1 tensor attention map by employing strip pooling on each chunk so that local and long-range contextual information can be captured along three dimension respectively; RDEM generates three 2D feature descriptors of the residual feature to produce the complement attention map, using three factor vectors of the initial attention map and three descriptors of the input feature. Extensive experimental results on ImageNet-1K, MS COCO and PASCAL VOC demonstrate that DRTAM achieves competitive performance on both large and mobile networks compare with other state-of-the-art attention modules.

Keywords: Attention mechanism, rank-1 tensor, residual-attention-learning

1 Introduction

Convolutional neural networks (CNNs) have been proven very effective in a broad range of computer vision tasks due to their powerful representation ability [15,23,18]. Traditional CNNs try to improve the representation ability by designing different modules to stack a deeper network[25,8,26]. Unfortunately, these deeper and wider networks bring in high computational cost despite that they can show more excellent performance.

Recently, attention mechanism, a component used to enhance the network performance, has been extensively investigated[13,32,31,5]. Different from traditional CNN designs, this component tries to tell a model "what" and "where" to

* Baihong Lin is the corresponding author.
E-mail: {linbh6@mail.sysu.edu.cn, linbaihong111@126.com}

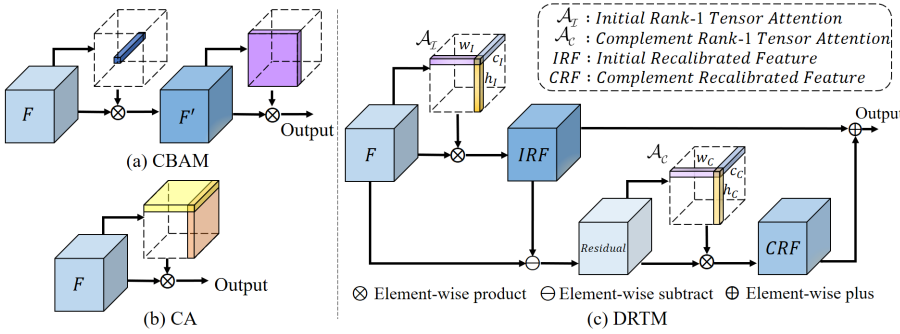

Fig. 1. Comparison for Module Architectures of CBAM[32], CA[10] and DRTAM.

attend instead of stacking modules so that the network representation ability can be improved efficiently[20,34]. So far, various attention mechanisms have been proposed, including SE-Net [13], CBAM-Net [32], BAM-Net [21], CA-Net [10] and etc. However, most of them are designed for large networks or mobile networks. Few attention mechanisms show excellent performance on large networks as well as mobile networks.

To design an efficient attention module for large and mobile networks, we deeply study two distinguished attention module in the recent years, including CBAM[32] and CA[10]. The architectures of CBAM and CA are shown in Fig.1. CBAM decomposes a 3D tensor attention map into a channel attention map and a spatial attention map. This attention module shows excellent performance on large networks. To generate the spatial attention map, this module employs average-pooling and max-pooling along the channel dimension, then concatenates them to produce a 2D spatial attention map by a convolution layer. However, the computational cost brought by convolution is redundant, since spatial attention is used to recalibrate certain spatial region of feature and usually does not have to carry too much image detail. Furthermore, it has been pointed out that attention maps generated by convolutions can only capture local relations but fail in modeling essential long-range dependencies[9,10]. As for CA, this module decomposes a 3D tensor attention map into two coordinate-aware attention maps, simplifying the spatial attention design by learning horizontal and vertical attention separately instead of directly computing a 2D spatial attention map[10]. Unfortunately, although long-range dependencies can be captured along one spatial direction in CA, local dependencies, which is also important for attention map generation, are neglected in this module design. Furthermore, our experiments show CA mainly works better on mobile networks but not large networks, and such attention module has higher computational cost than that of CBAM. Besides, both of CBAM and CA modules are plugged in every convolutional block, whether it is necessary or not, which brings in high computational cost compared with traditional networks without attention mechanisms.

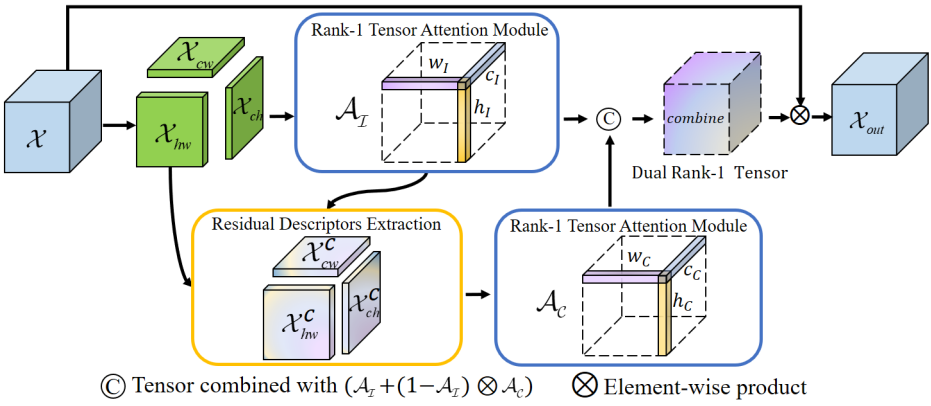

Fig. 2. The overview of proposed Dual Rank-1 Tensor Attention Module(DRTAM).

On the basis of the above studies, this paper proposes a novel and efficient attention module named *dual rank-1 tensor module* (DRTAM). Inspired by residual attention learning [8,29], DRTAM factorizes a 3D tensor attention map into two complement rank-1 3D tensor attention maps, named the initial rank-1 tensor attention map and the complement rank-1 tensor attention map, as illustrated in Fig.1. To generate two rank-1 tensor attention maps, we propose *rank-1 tensor attention module* and *residual descriptors extraction module*, as illustrated in Fig.2. Specifically, we first generate three 2D feature descriptors $\{\mathcal{X}_{cw}, \mathcal{X}_{ch}, \mathcal{X}_{hw}\}$ to represent a 3D feature tensor $\mathcal{X}$ and cut down the computational cost for further calculation of attention maps. Then, the initial rank-1 tensor attention map $\mathcal{A}_\mathcal{I}$ is generated by a rank-1 tensor attention module based on three 2D feature descriptors of an intermediate feature $\mathcal{X}$ in a network, whereas the complement rank-1 tensor attention map $\mathcal{A}_\mathcal{C}$ is generated by another rank-1 tensor attention module based on three 2D feature descriptors of the residual feature $\mathcal{X}-\mathcal{X}\otimes\mathcal{A}_\mathcal{I}$. To obtain three 2D feature descriptors of the residual feature, we propose the residual descriptors extraction module based on three 2D feature descriptors of the intermediate feature $\mathcal{X}$ and the initial rank-1 tensor attention map $\mathcal{A}_\mathcal{I}$. Finally, the initial rank-1 tensor attention map $\mathcal{A}_\mathcal{I}$ and the complement rank-1 tensor attention map $\mathcal{A}_\mathcal{C}$ are combined into an attention map to recalibrate the intermediate feature $\mathcal{X}$. Experiments show that DRTAM show relatively better performance on large and mobile networks, compare with other state-of-the-art attention modules.The contributions of this paper are summarized as three folds:

1. Inspired by residual attention learning[8,29], we design DRTAM that can be widely applied to boost representation power of large and mobile networks.
2. In DRTAM, we design rank-1 tensor attention module, which can utilize local and long-range contextual information to generate rank-1 attention map.
3. Extensive experimental results on ImageNet-1K, MS COCO and PASCAL VOC demonstrate that DRTAM has considerable model complexity with the

state-of-the-art attention module while achieving outstanding performance on large and mobile networks.

2 Related Work

Network Engineering In computer vision, well-designed deep convolutional neural network (CNN) can ensure excellent performance for different applications. Early researches focus on building a deeper network to enhance performance for image recognition and object detection. Starting with AlexNet [15], the exploration of deeper convolutional neural network is never stopped: VGG-Net [25] shows that stacking the same type of block into a deeper networks could significantly enhance vision performance. Inspired by VGG-Net, ResNet [8] and GoogleNet [26] propose stack residual modules and inception modules to stack a deeper network, respectively. Subsequently, researchers try to improve the network based on ResNet and GoogleNet, including ResNext [33], DenseNet [14], ResNeSt [36] and etc. However, although the above large networks show remarkable performance, they are not suitable for computation capacity restricted applications due to their high computational cost of parameters and floating point operations(FLOPs).

To facilitate implementation for computation capacity restricted cases like mobile devices or embedded systems, lightweight networks are designed: Specifically, MobileNetV1 [12] builds a lightweight network based on depthwise separable convolutions. Sequentially, MobileNetV2 [24] proposes inverted residual block to improve feature representation ability. MobileNetV3 [11] proposes network architecture search (NAS) and NetAdapt algorithm to automatically search the most effective model for a specific vision task. To further simplify MobileNet, ShuffleNetV1 [37] proposes pointwise group convolution and channel shuffle operation to reduce network parameters and maintain the information interaction across feature channels respectively. Later, ShuffleNetV2 [19] enhances the performance of ShuffleNetV1 by appending channel split operation in each inverted residual block base on ShuffleNetV1. Moverover, EfficientNet [27], MicroNet [17] and GhostNet [6] try to explore other strategies to reduce the network computational complexity and enhance the corresponding performance. All these designs help to promote the development of lightweight networks.

Attention Mechanisms In recent years, attention mechanism, a component used to enhance the network performance, has been extensively investigated[13,32,31,5]. This component can help to recalibrate feature, i.e., focusing on interesting features while suppressing noisy with extra low computational cost, thus, it wins many researchers' attention.

Self-attention have been widely applied due to their capability of building long-range dependencies [28,31,20]. This kind of attention module calculate attention map base on non-local block, which is proposed by Non-local neural networks [31]. Typical examples include *e.g.* A^2-Net [2], DA-Net [5] and etc.

However, although they push great improvement in networks, they are not suitable for lightweight networks due to considerable computational burden brought by non-local mechanisms. Meanwhile, compact attention modules are also under investigated. For instance, SE-Net [13] proposes a channel attention module to recalibrate feature channel by channel. On the basis of SE-Net, CBAM-Net [32] and BAM-Net [21] further introduce spatial attention module to recalibrate feature spatially with different network architectures. Later works, ECA-Net [30] implements 1D convolution to realize local cross-channel interaction, avoiding the dimensionality reduction of channel. SK-Net [16] allows network to adaptively adjust receptive field size. CA-Net [10] encodes positional information by strip pooling [9] and generates coordinate attention. These networks bring in better performance on visual tasks with lower computational complexity, compared with self-attention networks. However, most of these attention modules are difficult to keep distinctive performance in both deep neural networks and light-weight mobile networks.

Our work is based on CBAM-Net and CA-Net. Different from above-mentioned attention modules, this paper tries to design a universal attention module which can show stable and excellent performance in both deep neural networks and light-weight mobile networks with low computational cost.

3 Dual Rank-1 Tensor Attention Module

Let $\mathcal{X} \in \mathbb{R}^{C\times H\times W}$ denote an intermediate feature. Inspired by residual attention learning network[8,29], DRTAM sequentially infers two rank-1 tensor attention maps, the initial rank-1 tensor attention(IRTA) map denoted by $\mathcal{A}_{\mathcal{I}} \in \mathbb{R}^{C\times H\times W}$ and the complement rank-1 tensor attention map(CRTA) denoted by $\mathcal{A}_{\mathcal{C}} \in \mathbb{R}^{C\times H\times W}$, as illustrated in Fig.2. The overall attention process can be summarized as:

$$\begin{aligned}\mathcal{X}_{out} &= \mathcal{X} \otimes \mathcal{A}_{\mathcal{I}} + [\mathcal{X} \otimes (1 - \mathcal{A}_{\mathcal{I}})] \otimes \mathcal{A}_{\mathcal{C}} \\ &= \mathcal{X} \otimes (\mathcal{A}_{\mathcal{I}} + (1 - \mathcal{A}_{\mathcal{I}}) \otimes \mathcal{A}_{\mathcal{C}})\end{aligned} \tag{1}$$

where $\otimes$ denotes element-wise product, $\mathcal{X}_{out}$ denotes the final recalibrated feature. Obviously, $\mathcal{X} \otimes \mathcal{A}_{\mathcal{I}}$ denotes the initial recalibrated feature. $\mathcal{X} \otimes (1 - \mathcal{A}_{\mathcal{I}})$ represents the residual of the initial recalibrated feature. $\mathcal{A}_{\mathcal{C}}$ is introduced to recalibrate the residual $\mathcal{X}\otimes(1-\mathcal{A}_{\mathcal{I}})$, and obtain useful components to complement the initial recalibrated feature.

To generate all attention maps, we first obtain three feature descriptors $\mathcal{X}_{cw} \in \mathbb{R}^{C\times 1\times W}$, $\mathcal{X}_{ch} \in \mathbb{R}^{C\times H\times 1}$ and $\mathcal{X}_{hw} \in \mathbb{R}^{1\times H\times W}$ by employing average pooling on $\mathcal{X}$ along the horizontal, vertical and channel coordinates, respectively. Assuming that $\{\mathcal{X}_{cw}, \mathcal{X}_{ch}, \mathcal{X}_{hw}\}$ can well represent $\mathcal{X}$, operations on $\mathcal{X}$ will be replaced by operations on three feature descriptors to reduce the computational complexity of DRTAM. Then, on the basis of three feature descriptors $\{\mathcal{X}_{cw}, \mathcal{X}_{ch}, \mathcal{X}_{hw}\}$, we propose *rank-1 tensor attention module* and *residual descriptors extraction module* to generate $\mathcal{A}_{\mathcal{I}}$ and $\mathcal{A}_{\mathcal{C}}$. The details of these two modules are described as follow.

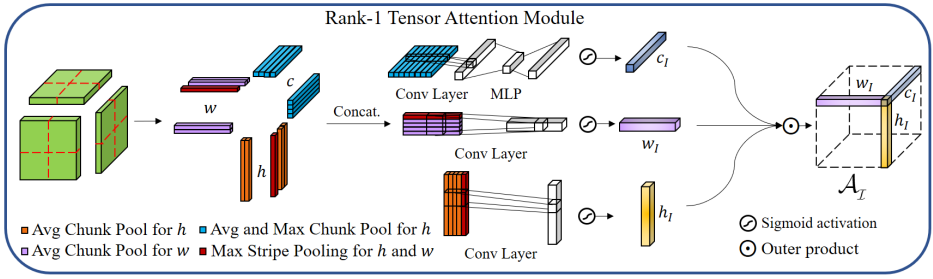

Fig. 3. Diagram of Rank-1 Tensor Attention Module to generate Initial (Complement) Rank-1 Tensor Attention map.

3.1 Rank-1 Tensor Attention Module

According to Canonical Polyadic (CP) Decomposition, a rank-1 tensor attention map $\mathcal{A}_{\mathcal{I}}$ can be decomposed into three vectors as the following:

$$\mathcal{A}_{\mathcal{I}} = c_I \circ h_I \circ w_I \tag{2}$$

where $\circ$ denotes outer product operation, $c_I \in \mathbb{R}^C$ denotes channel information embedding, $h_I \in \mathbb{R}^H$ and $w_I \in \mathbb{R}^W$ denote spatial information embedding vectors along vertical and horizontal coordinates respectively. The *rank-1 tensor attention module* transforms three 2D feature descriptors $\{\mathcal{X}_{cw}, \mathcal{X}_{ch}, \mathcal{X}_{hw}\}$ of a 3D feature tensor $\mathcal{X}$ into three decomposition embedding vectors of a rank-1 tensor attention map, as illustrated in Fig.3. In the following, we will introduce the generation process of channel information embedding and spatial information embedding in details.

Channel Information Embedding We produce the channel information embedding $c_I \in \mathbb{R}^C$ based on two 2D feature descriptors $\{\mathcal{X}_{cw}, \mathcal{X}_{ch}\}$. Apparently, the channel information embedding c_I can be regarded as channel attention map, which captures channel interaction and guide network to perceive the informative channels [13]. As has been proven, global avg-pooling and max-pooling can obtain long-range dependencies to generate better channel attention[32], whereas strip pooling can effectively capture long-range contextual information[9]. However, these two kinds of pooling layer sacrifice too much local contextual information, which is also importance for channel attention generation.

In our module, to jointly utilize local and long-range contextual information, we split feature descriptors $\mathcal{X}_{cw}$ and $\mathcal{X}_{ch}$ along H and W axes respectively into S chunks, denoted by $\{\mathcal{X}^i_{cw} \in \mathbb{R}^{C\times 1\times \frac{W}{S}}, i = 1, 2, ..., S\}$ and $\{\mathcal{X}^i_{ch} \in \mathbb{R}^{C\times \frac{H}{S}\times 1}, i = 1, 2, ..., S\}$. S is a hyperparameter which will be discuss in experiments. Then, we introduce strip avg-pooling and strip max-pooling for each chunk, and formulate

the pooling results as follow:

$$\mathcal{P}_{cw}^{k}(\text{Avg},\text{Max}) = \left[\frac{S}{W} \sum_{j=\frac{(k-1)W+S}{S}}^{\frac{kW}{S}} \mathcal{X}_{cw}^{k}(:,1,j)\,,\ \max_{\frac{(k-1)W}{S}<j\leq\frac{kW}{S}} \left(\mathcal{X}_{cw}^{k}(:,1,j)\right) \right] \tag{3}$$

$$\mathcal{P}_{ch}^{k}(\text{Avg},\text{Max}) = \left[\frac{S}{H} \sum_{j=\frac{(k-1)H+S}{S}}^{\frac{kH}{S}} \mathcal{X}_{ch}^{k}(:,j,1)\,,\ \max_{\frac{(k-1)H}{S}<j\leq\frac{kH}{S}} \left(\mathcal{X}_{ch}^{k}(:,j,1)\right) \right] \tag{4}$$

where $\mathcal{P}_{cw}^{k}(\text{Avg},\text{Max}) \in \mathbb{R}^{C\times 2}$ and $\mathcal{P}_{ch}^{k}(\text{Avg},\text{Max}) \in \mathbb{R}^{C\times 2}$ denote the pooling results containing local and long-range contextual information, $k = 1, 2, ..., S$. Then, we concatenate the pooling results into $\mathcal{P}_c \in \mathbb{R}^{C\times 4S}$ and adopt a 2D convolution layer with kernel (1,4S) to integrate a sufficient descriptor $\mathcal{S}_c \in \mathbb{R}^{C\times 1}$, which contains all channel information in $\mathcal{X}$:

$$\begin{aligned}\mathcal{S}_c = \text{Conv2D}(\mathcal{P}_c) = \text{Conv2D}([&\mathcal{P}_{cw}^{1}(\text{Avg},\text{Max}), \mathcal{P}_{ch}^{1}(\text{Avg},\text{Max}),\\ &..., \mathcal{P}_{cw}^{S}(\text{Avg},\text{Max}), \mathcal{P}_{ch}^{S}(\text{Avg},\text{Max})])\end{aligned} \tag{5}$$

Finally, the descriptor $\mathcal{S}_c \in \mathbb{R}^{C\times 1}$ is forwarded to a multi-layer perceptron (MLP) network with one hidden layer to produce the channel information embedding $c_I \in \mathbb{R}^{C}$:

$$c_I = \sigma(\mathcal{F}_1(\mathcal{F}_0(\mathcal{S}^c))) \tag{6}$$

where $\sigma(\cdot)$ denotes the sigmoid function, $\mathcal{F}_0 \in \mathbb{R}^{C\times C/r}$ and $\mathcal{F}_1 \in \mathbb{R}^{C/r\times C}$ are two fully-connected layers to transform $\mathcal{S}^c \in \mathbb{R}^{C\times 1}$ into $c_I \in \mathbb{R}^{C}$.

Spatial Information Embedding We produce the spatial information embedding $h_I \in \mathbb{R}^{H}$ and $w_I \in \mathbb{R}^{W}$ based on $\{\mathcal{X}_{ch}, \mathcal{X}_{hw}\}$ and $\{\mathcal{X}_{cw}, \mathcal{X}_{hw}\}$, respectively. Obviously, $h_I \circ w_I$ can be regarded as spatial attention map, which captures spatial correlation and guide network to perceive the informative spatial parts. Most of spatial attention modules directly extract informative texture from these intricated feature descriptor by implementing a standard convolution layer[35,32]. However, a single convolution layer can only capture neighbor contextual information, which will neglect long-range contextual information.

In our module, similar to the generation of channel information embedding, we split feature descriptors into chunks to jointly utilize local and long-range contextual information for spatial information embedding generation. Take the generation of $h_I \in \mathbb{R}^{H}$ for example, we firstly split $\mathcal{X}_{hw}$ along W axis into S chunks denoted by $\{\mathcal{X}_{hw}^{k}, k = 1, 2, ..., S\}$, and split $\mathcal{X}_{ch}$ along C channel axis into N chunks denoted by $\{\mathcal{X}_{ch}^{n}, n = 1, 2, ..., N\}$. Then, we introduce strip avg-pooling

for each chunk, and formulate the pooling results as follow:

$$\mathcal{P}_{hw}^{k}(\text{Avg}) = \frac{S}{W}\sum_{j=1}^{W/S}\mathcal{X}_{hw}^{k}\left(1,:,j+(k-1)\frac{W}{S}\right) \tag{7}$$

$$\mathcal{P}_{ch}^{n}(\text{Avg}) = \frac{N}{C}\sum_{j=1}^{C/N}\mathcal{X}_{ch}^{n}\left(j+(k-1)\frac{C}{N},:,1\right) \tag{8}$$

where $\mathcal{P}_{hw}^{k}(\text{Avg}) \in \mathbb{R}^{H\times 1}$ and $\mathcal{P}_{ch}^{n}(\text{Avg}) \in \mathbb{R}^{H\times 1}$ denote the pooling results containing local and long-range contextual information, $k = 1, 2, ..., S$, $n = 1, 2, ..., N$. Instead of introducing strip max-pooling for each chunk, we introduce strip max-pooling on $\mathcal{X}_{ch}$, the results can be formulated as the following:

$$\overline{\mathcal{P}}_{ch}(\text{Max}) = \max_{0<j\leq C}\left(\mathcal{X}_{ch}\left(j,1,:\right)\right) \tag{9}$$

where $\overline{P}_{ch}(\text{Max}) \in \mathbb{R}^{H\times 1}$ denote the pooling results containing global contextual information. Then, we concatenate all pooling results into $\mathcal{P}_h \in \mathbb{R}^{H\times(S+N+1)}$ and adopt a 2D convolution layer with kernel $(3, S+N+1)$ to integrate a sufficient descriptor $\mathcal{S}_h \in \mathbb{R}^{H\times 1}$, which contains all H-axis information in $\mathcal{X}$:

$$\begin{aligned}\mathcal{S}_h = \text{Conv2D}(\mathcal{P}_h) = \text{Conv2D}([&\mathcal{P}_{hw}^{1}(\text{Avg}), \mathcal{P}_{ch}^{1}(\text{Avg}),\\ &..., \mathcal{P}_{hw}^{S}(\text{Avg}), \mathcal{P}_{ch}^{N}(\text{Avg}), \overline{\mathcal{P}}_{ch}(\text{Max})])\end{aligned} \tag{10}$$

Finally, the descriptor $\mathcal{S}_h \in \mathbb{R}^{H\times 1}$ is forwarded to batch normalization (BN) layer and the sigmoid function $\sigma(\cdot)$ to produce the spatial information embedding h_I:

$$h_I = \sigma(\text{BN}(\mathcal{S}^h)) \tag{11}$$

The above passage only introduces the generation of $h_I \in \mathbb{R}^H$. But the generation of $w_I \in \mathbb{R}^W$ is similar to the generation of $h_I \in \mathbb{R}^H$. We can obtain $w_I \in \mathbb{R}^W$ by substituting H-axis with W-axis in the generation process of h_I.

Arrangement of Attention Modules As illustrated in Fig.2, given a 3D feature tensor $\mathcal{X}$, $\mathcal{A}_\mathcal{I}$ is generated from three feature descriptors $\{\mathcal{X}_{ch}, \mathcal{X}_{cw}, \mathcal{X}_{hw}\}$ of $\mathcal{X}$ using a rank-1 tensor attention module, whereas $\mathcal{A}_\mathcal{C}$ is generated from three feature descriptors $\{\mathcal{X}_{ch}^{C}, \mathcal{X}_{cw}^{C}, \mathcal{X}_{hw}^{C}\}$ of $\mathcal{X}\otimes(1-\mathcal{A}_\mathcal{I})$ using another rank-1 tensor attention module. Obviously, two rank-1 tensor attention modules are introduce to generate $\mathcal{A}_\mathcal{I}$ and $\mathcal{A}_\mathcal{C}$. Both of these two attention modules try to transform a feature into an attention map. Thus, to cut down the computational complexity, we share some parameters in two rank-1 tensor attention modules, e.g. the parameters of two fully-connected layers $\mathcal{F}_0$ and $\mathcal{F}_1$ in Eqn.(6).

3.2 Residual Descriptors Extraction Module

Although $\{\mathcal{X}_{ch}^{C}, \mathcal{X}_{cw}^{C}, \mathcal{X}_{hw}^{C}\}$ can be obtained by employing avg-pooling on $\mathcal{X}\otimes(1-\mathcal{A}_\mathcal{I})$, this calculation features the complexity $\mathcal{O}(HWC)$, and will bring in

high computational cost. Therefore, instead of directly employing avg-pooling on $\mathcal{X} \otimes (1 - \mathcal{A}_{\mathcal{I}})$, we propose residual descriptors extraction module to obtain $\{\mathcal{X}^C_{ch}, \mathcal{X}^C_{cw}, \mathcal{X}^C_{hw}\}$. In the residual descriptors extraction module, feature descriptors $\{\mathcal{X}^C_{ch}, \mathcal{X}^C_{cw}, \mathcal{X}^C_{hw}\}$ are obtained based on feature descriptors $\{\mathcal{X}_{ch}, \mathcal{X}_{cw}, \mathcal{X}_{hw}\}$ of $\mathcal{X}$ and the CP decomposition vectors $\{c_I, h_I, w_I\}$ of $\mathcal{A}_{\mathcal{I}}$ as follow:

$$\mathcal{X}^C_{ch} = \text{AvgPool}_W(\mathcal{X} \otimes (\mathbf{1} - c_I \circ h_I \circ \mathbf{1})) = \mathcal{X}_{ch} \otimes (\mathbf{1} - c_I \circ h_I) \tag{12}$$

$$\mathcal{X}^C_{cw} = \text{AvgPool}_H(\mathcal{X} \otimes (\mathbf{1} - c_I \circ \mathbf{1} \circ w_I)) = \mathcal{X}_{cw} \otimes (\mathbf{1} - c_I \circ w_I) \tag{13}$$

$$\mathcal{X}^C_{hw} = \text{AvgPool}_C(\mathcal{X} \otimes (\mathbf{1} - \mathbf{1} \circ h_I \circ w_I)) = \mathcal{X}_{hw} \otimes (\mathbf{1} - h_I \circ w_I) \tag{14}$$

where $\mathbf{1}$ denotes an all-one vector or an all-one matrix, $\circ$ denotes outer product operation, $\otimes$ denotes element-wise product, $\text{AvgPool}_W(\cdot)$ denotes avg-pooling operation along W-axis. The above calculation features relatively lower complexity $\mathcal{O}(HW + WC + HC)$. Obviously, feature descriptors $\{\mathcal{X}^C_{ch}, \mathcal{X}^C_{cw}, \mathcal{X}^C_{hw}\}$ generated by residual descriptors extraction module are different from feature descriptors $\{\mathcal{X}'^C_{ch}, \mathcal{X}'^C_{cw}, \mathcal{X}'^C_{hw}\}$ generated by employing avg-pooling on $\mathcal{X} \otimes (1 - \mathcal{A}_{\mathcal{I}})$. But $\{\mathcal{X}^C_{ch}, \mathcal{X}^C_{cw}, \mathcal{X}^C_{hw}\}$ can be regarded as an approximation of $\{\mathcal{X}'^C_{ch}, \mathcal{X}'^C_{cw}, \mathcal{X}'^C_{hw}\}$, since $c_I \circ h_I \circ \mathbf{1}$, $c_I \circ \mathbf{1} \circ w_I$ and $\mathbf{1} \circ h_I \circ w_I$ in Eqn.(12)-Eqn.(14) are approximations of $\mathcal{A}_{\mathcal{I}} = c_I \circ h_I \circ w_I$. On the basis of the residual descriptors extraction module, $\{\mathcal{X}^C_{ch}, \mathcal{X}^C_{cw}, \mathcal{X}^C_{hw}\}$ and $\mathcal{A}_{\mathcal{C}}$ can be obtained with lower computational cost.

4 Experiments

In this section, we first explain the fundamental settings in our experiment. To analyze the effection of each structure in DRTAM, we perform a series of ablation experiments. Finally, we compare DRTAM with state-of-the-art attention modules on ImageNet-1K dataset for image classification, COCO dataset for object Detection and segmentation, and VOC dataset for semantic segmentation to reflect the general applicability of DRTAM.

4.1 Experiments Setup

All experiments are conducted based on MMClassification toolbox [3] and PyTorch [22]. We take ResNet [8] and MobileNetV2 [24] as our baseline and train all comparison models for 100 and 300 epochs respectively. Then, we set the minibatch size and the initial learning rate to 64 and 0.045 respectively for MobileNetV2-1.0 and MobileNetV2-0.5, set the minibatch size and the initial learning rate to 128 and 0.2 respectively for ResNet-50, and set the minibatch size and the initial learning rate to 96 and 0.2 respectively for ResNet-101. During training, we use the standard SGD optimizer with momentum of 0.9, and set the weight decay to 1×10^{-4} and 4×10^{-5} for ResNet and MobileNetV2 respectively. For fair comparison, the same data augmentation methods and the single-crop with size of 224×224 are adopted at training and testing pipeline. Besides, For ResNet, we plug all attention module following by bottelneck. For MobileNetV2, we plug attention module following by every invert bottelneck.

Table 1. The influence of S based on ResNet-50 and MobileNetV2-1.0.

Backbone	Param.	GFlops	S	N	Top-1 (%)	Top-5 (%)
ResNet-50	25.56 M	4.12	-	-	76.432	93.032
+ DRTAM	26.83 M	4.14	2	1	77.184	**93.620**
+ DRTAM	26.83 M	4.14	3	1	**77.366**	93.560
+ DRTAM	26.83 M	4.14	4	1	76.984	93.478
MobileNetV2-1.0	3.50 M	0.32	-	-	71.592	90.380
+ DRTAM	3.80 M	0.33	2	1	72.930	91.118
+ DRTAM	3.80 M	0.33	3	1	**73.084**	**91.170**
+ DRTAM	3.80 M	0.33	4	1	72.854	91.067

Table 2. The influence of N based on ResNet-50 and MobileNetV2-1.0.

Backbone	Param.	GFlops	N	S	Top-1 (%)	Top-5 (%)
ResNet-50	25.56 M	4.12	-	-	76.432	93.032
+ DRTAM	26.83 M	4.14	1	3	**77.366**	93.560
+ DRTAM	26.83 M	4.14	2	3	76.960	93.552
+ DRTAM	26.83 M	4.14	4	3	77.286	**93.584**
MobileNetV2-1.0	3.50 M	0.32	-	-	71.592	90.380
+ DRTAM	3.80 M	0.33	1	3	73.084	**91.170**
+ DRTAM	3.80 M	0.33	2	3	72.858	90.988
+ DRTAM	3.80 M	0.33	4	3	**73.140**	90.974
+ DRTAM	3.80 M	0.33	8	3	73.130	90.948

On the basis of the above setting, we use four NVIDIA GPUs for model training and report the corresponding testing results on different datasets.

4.2 Ablation Study

In this section, we conduct a group of comparison experiments to empirically exploit the effectiveness of our attention module. The design of DRTAM involves three hyper-parameters $\{S, N, r\}$: S denotes the number of chunks along H-axis and W-axis in Eqn.(3), Eqn.(4) and Eqn.(7); N denotes the number of chunks along C-axis in Eqn.(8); r denotes the reduction ratio of the MLP network in Eqn.(6). In the following passage, we sequentially explore the influence of S, the influence of N and the influence of r. The analyses are shown as the following.

The influence of S. We fix $N = 1$ and $r = 32$, then, we explore the influence of S by taking ResNet-50 and MobileNetV2-1.0 as baseline. The corresponding experiment results are shown in Table.1. It can be found that DRTAM shows the best performance for ResNet-50 and MobileNetV2-1.0 under Top-1 accuracy

Table 3. The influence of r based on ResNet50, ResNet101 and MobileNetV2-1.0.

Backbone	Attention	Param.	GFlops	r	S	N	Top-1 (%)	Top-5 (%)
ResNet-50	DRTAM	26.83 M	4.14	32	3	1	**77.366**	93.560
		28.09 M	4.15	16	3	1	77.172	93.460
ResNet-101	DRTAM	46.96 M	7.89	32	3	1	77.946	94.000
		49.33 M	7.89	16	3	1	**78.234**	93.914
MobileNetV2-1.0	DRTAM	3.80 M	0.33	32	3	4	**73.140**	90.974
		4.08 M	0.33	16	3	4	73.040	91.080

when S is set to 3. Beside, it seems that the best value of S have no relation to network complexity, i.e., the best value of S is the same for large and mobile networks.

The influence of N. We fix $S = 3$ and $r = 32$, then, we explore the influence of N by taking ResNet-50 and MobileNetV2-1.0 as baseline. The corresponding experiment results are shown in Table.2. It can be found that DRTAM shows the best performance under Top-1 accuracy when $N = 1$ for ResNet-50 and $N = 4$ for MobileNetV2-1.0. Obviously, the value of N is related to network complexity, i.e., the best value of N is not the same for large and mobile networks.

The influence of r. We fix $N = 1$ and $S = 3$ for ResNet, and fix $N = 4$ and $S = 3$ for MobileNetV2, then, we explore the influence of r by taking ResNet-50, ResNet-101 and MobileNetV2-1.0 as baseline. The corresponding experiment results are shown in Table.3. It can be found that DRTAM shows the best performance under Top-1 accuracy when $r = 32$ for ResNet-50 and MobileNetV2-1.0, and $r = 16$ for ResNet-101. Obviously, the setting of r depend on the complexity of network, i.e., the best value of r tend to be large when the baseline network has higher computational complexity.

On the basis of the above ablation study, we set $S = 3$ and $N = 1$ for ResNet, and set $S = 3$ and $N = 4$ for MobileNetV2. As for the hyperparameter r, we only set it to 16 for ResNet-101, otherwise, we tend to set r to 32.

4.3 Comparison on ImageNet-1K classification

We take ResNet and MobileNetV2 as baseline, and compare DRTAM with two state-of-the-art attention modules, CBAM[32] and CA[10], on ImageNet-1K dataset in classification. The experiment results are shown in Table 4.

It can be found that DRTAM show the best performance under Top-1 accuracy when $r = 32$ for ResNet-50 and MobileNetV2, and $r = 16$ for ResNet-101. Besides, the performance of DRTAM show relatively stable compared with CBAM and CA on large and mobile networks. As for other comparison attention modules, CBAM shows relatively excellent performance on ResNet, but it turns

Table 4. Comparison of state-of-the-art attention methods on ImageNet.

Model	Param.	GFlops	r	Top-1 (%)	Top-5 (%)
ResNet50	25.56 M	4.12	-	76.432	93.032
+ CBAM	**26.83 M**	**4.12**	32	77.100	93.388
+ CBAM	28.09 M	4.14	16	77.188	**93.584**
+ CA	27.47 M	4.16	32	76.736	93.260
+ CA	29.36 M	4.19	16	76.900	93.356
+ DRTAM	**26.83 M**	4.14	32	**77.366**	93.560
+ DRTAM	28.09 M	4.15	16	77.172	93.460
ResNet101	44.55 M	7.85	-	77.856	93.778
+ CBAM	**46.96 M**	**7.85**	32	78.042	93.858
+ CBAM	49.33 M	7.88	16	78.118	94.020
+ CA	48.17 M	7.92	32	77.960	**94.062**
+ CA	51.74 M	7.98	16	77.908	94.020
+ DRTAM	**46.96 M**	7.89	32	77.946	94.000
+ DRTAM	49.33 M	7.89	16	**78.234**	93.914
MobileNetV2-1.0	3.50 M	0.32	-	71.592	90.380
+ CBAM	4.08 M	**0.32**	16	72.924	90.968
+ CA	3.95 M	0.33	32	73.034	**91.106**
+ DRTAM	**3.80 M**	0.33	32	**73.140**	90.974
MobileNetV2-0.75	2.64 M	0.22	-	69.442	88.814
+ CBAM	2.96 M	0.23	16	71.404	90.058
+ CA	2.89 M	0.23	32	71.206	90.086
+ DRTAM	**2.81 M**	**0.23**	32	**71.468**	**90.088**

unstable for mobile networks, and shows worst performance on MobileNetV2-1.0. CA performs worst on ResNet, but better on MobileNetV2, especially on MobileNetV2-1.0.

As for parameters and GFLOPs, DRTAM shares the nearly same index values as that of CBAM on ResNet, but features the lowest on MobileNetV2. CBAM features the lowest GFLOPs in most cases, but higher index values for parameters. CA features less parameters on ResNet, but it results in higher GFLOPs on ResNet. In summary, comparing with other attention modules, DRTAM shows excellent performance in classification on the large-scale dataset, but consuming relatively lower model complexity.

4.4 Comparison on MS COCO Object Detection and Segmentation

For fair comparison on MS COCO dataset in object detection and segmentation, we adopt Mask R-CNN as detector, use pre-trained ResNet-50 and ResNet-101 provided by PyTorch to initiate all backbones, and train all detectors following

Table 5. Object detection results on COCO val2017 set with Mask R-CNN.

Backbone	Param.	GFlops	AP	AP_{50}	AP_{75}	AP_S	AP_M	AP_L
ResNet-50	44.18 M	76.86	38.0	58.6	41.3	21.8	41.9	49.3
+ CA	**46.08 M**	76.90	38.5	59.1	41.8	22.1	42.1	50.4
+ DRTAM	46.69 M	**76.88**	**38.7**	**59.3**	**41.8**	**22.2**	**42.1**	**50.9**
ResNet-101	63.17 M	80.59	40.0	60.4	43.2	23.3	44.2	52.6
+ CA	**66.78 M**	80.66	40.1	60.6	43.5	23.1	44.2	52.4
+ DRTAM	67.93 M	**80.63**	**40.8**	**61.6**	**44.4**	**23.5**	**44.8**	**53.6**

Table 6. Semantic segmentation results on COCO val2017 set with Mask-RCNN.

Backbone	AP	AP_{50}	AP_{75}	AP_S	AP_M	AP_L
ResNet-50	34.3	55.1	36.6	18.2	37.7	46.6
+ CA	34.6	55.7	**37.0**	18.3	37.9	47.2
+ DRTAM	**34.7**	**56.1**	36.9	**18.3**	**38.0**	**47.6**
ResNet-101	35.8	57.1	38.2	19.3	39.7	49.1
+ CA	35.9	57.4	38.2	**19.3**	39.5	49.2
+ DRTAM	**36.4**	**58.2**	**38.9**	19.2	**40.1**	**50.2**

Table 7. Semantic segmentation results on PASCAL VOC 2012 set with FCN.

Backbone	Param. (Bott./Pool.)	GFlops (Bott./Pool.)	mIoU (Bott./Pool.)
ResNet-50	49.48 M	196.47	67.68
+ CBAM	52.01 / 50.18 M	**196.49 / 196.48**	74.46 / 74.40
+ CA	51.40 / 50.01 M	196.78 / 196.57	73.11 / 73.63
+ DRTAM($r = 32$)	**50.75 / 49.83 M**	196.71 / 196.55	**75.47 / 74.84**
ResNet-101	68.47 M	274.16	71.21
+ CBAM	73.25 / 69.17 M	**274.18 / 274.17**	**77.27** / 75.98
+ CA	**72.10 / 69.00 M**	274.75 / 274.25	74.84 / 76.23
+ DRTAM($r = 16$)	73.25 / 69.17 M	274.63 / 274.23	76.61 / **76.70**

the MMDetection toolkit [1] under default settings. The results are shown in Table.5 and Table.6, It can be found that DRTAM outperforms CA in most index values, which proves the superiority of DRTAM on COCO dataset in object detection and segmentation.

4.5 Comparison on VOC 2012 Semantic Segmentation

Most recent works on Pascal VOC 2012 dataset usually exploit extra augmentation data, thus, we augment the training set from [7], which prepared totally

11355 for training and 1446 for valuating. On the basis of the augmentation VOC dataset, we conduct experiments on instance segmentation using MMSegmentation toolkit [4] under default settings. The experiment results are shown in Table.7, in which "Bott./Pool." denotes pluging an attention module following every bottleneck or every pooling layer in ResNet architecture.

From Table.7, It can be found that DRTAM shows the best performance on ResNet-50 while CBAM shows the best performance on ResNet-101. In addition, we find that attention module plugged following pooling layer can reduce considerable model parameter and GFlops, but can still achieve competitive result.

5 conclusion

In this paper, we propose Dual Rank-1 Tensor Attention Module (DRTAM) for convolutional neural networks based on residual attention learning. Specifically, DRTAM firstly generates three 2D feature descriptors along three axes. Then, using three descriptors, DRTAM sequentially infers two rank-1 tensor attention maps, the initial attention map and the complement attention map, combines and multiplied them to the input feature map for adaptive feature refinement. To generate two attention maps, DRTAM introduces rank-1 tensor attention module (RTAM) and residual descriptors extraction module (RDEM), in which local and long range dependencies are utilized for rank-1 attention generation and 2D feature descriptors of residual feature are generated, respectively. Extensive experimental results are conducted on ImageNet-1K, MS COCO and PASCAL VOC datasets, which demonstrate that DRTAM shows excellent performance but consuming relatively lower model complexity on large and mobile networks compare with other state-of-the-art attention modules.

6 Acknowledgement

The work is supported in part by the Science Technology and Innovation Commission of Shenzhen Municipality under Grant 2021A03, in part by the Fundamental Research Funds for the Central Universities(Sun Yat-sen University) under Grant 2021qntd11.

References

1. Chen, K., Wang, J., Pang, J., Cao, Y., Xiong, Y., Li, X., Sun, S., Feng, W., Liu, Z., Xu, J., et al.: Mmdetection: Open mmlab detection toolbox and benchmark. arXiv preprint arXiv:1906.07155 (2019)
2. Chen, Y., Kalantidis, Y., Li, J., Yan, S., Feng, J.: a^2-nets: Double attention networks. arXiv preprint arXiv:1810.11579 (2018)
3. Contributors, M.: Openmmlab's image classification toolbox and benchmark. `https://github.com/open-mmlab/mmclassification` (2020)
4. Contributors, M.: MMSegmentation: Openmmlab semantic segmentation toolbox and benchmark. `https://github.com/open-mmlab/mmsegmentation` (2020)
5. Fu, J., Liu, J., Tian, H., Li, Y., Bao, Y., Fang, Z., Lu, H.: Dual attention network for scene segmentation. In: Proceedings of the IEEE/CVF Conference on Computer Vision and Pattern Recognition. pp. 3146–3154 (2019)
6. Han, K., Wang, Y., Tian, Q., Guo, J., Xu, C., Xu, C.: Ghostnet: More features from cheap operations. In: Proceedings of the IEEE/CVF Conference on Computer Vision and Pattern Recognition. pp. 1580–1589 (2020)
7. Hariharan, B., Arbeláez, P., Bourdev, L.D., Maji, S., Malik, J.: Semantic contours from inverse detectors. 2011 International Conference on Computer Vision pp. 991–998 (2011)
8. He, K., Zhang, X., Ren, S., Sun, J.: Deep residual learning for image recognition. In: Proceedings of the IEEE conference on computer vision and pattern recognition. pp. 770–778 (2016)
9. Hou, Q., Zhang, L., Cheng, M.M., Feng, J.: Strip pooling: Rethinking spatial pooling for scene parsing. 2020 IEEE/CVF Conference on Computer Vision and Pattern Recognition (CVPR) (2020)
10. Hou, Q., Zhou, D., Feng, J.: Coordinate attention for efficient mobile network design. In: Proceedings of the IEEE/CVF Conference on Computer Vision and Pattern Recognition. pp. 13713–13722 (2021)
11. Howard, A., Sandler, M., Chu, G., Chen, L.C., Chen, B., Tan, M., Wang, W., Zhu, Y., Pang, R., Vasudevan, V., et al.: Searching for mobilenetv3. In: Proceedings of the IEEE/CVF International Conference on Computer Vision. pp. 1314–1324 (2019)
12. Howard, A.G., Zhu, M., Chen, B., Kalenichenko, D., Wang, W., Weyand, T., Andreetto, M., Adam, H.: Mobilenets: Efficient convolutional neural networks for mobile vision applications. arXiv preprint arXiv:1704.04861 (2017)
13. Hu, J., Shen, L., Sun, G.: Squeeze-and-excitation networks. In: Proceedings of the IEEE conference on computer vision and pattern recognition. pp. 7132–7141 (2018)
14. Huang, G., Liu, Z., Van Der Maaten, L., Weinberger, K.Q.: Densely connected convolutional networks. In: Proceedings of the IEEE conference on computer vision and pattern recognition. pp. 4700–4708 (2017)
15. Krizhevsky, A., Sutskever, I., Hinton, G.E.: Imagenet classification with deep convolutional neural networks. Advances in neural information processing systems **25**, 1097–1105 (2012)
16. Li, X., Wang, W., Hu, X., Yang, J.: Selective kernel networks. In: Proceedings of the IEEE/CVF Conference on Computer Vision and Pattern Recognition. pp. 510–519 (2019)
17. Li, Y., Chen, Y., Dai, X., Chen, D., Liu, M., Yuan, L., Liu, Z., Zhang, L., Vasconcelos, N.: Micronet: Improving image recognition with extremely low flops. In: Proceedings of the IEEE/CVF International Conference on Computer Vision. pp. 468–477 (2021)

18. Long, J., Shelhamer, E., Darrell, T.: Fully convolutional networks for semantic segmentation. In: Proceedings of the IEEE conference on computer vision and pattern recognition. pp. 3431–3440 (2015)
19. Ma, N., Zhang, X., Zheng, H.T., Sun, J.: Shufflenet v2: Practical guidelines for efficient cnn architecture design. In: Proceedings of the European conference on computer vision (ECCV). pp. 116–131 (2018)
20. Mnih, V., Heess, N., Graves, A., Kavukcuoglu, K.: Recurrent models of visual attention. Advances in Neural Information Processing Systems **3** (2014)
21. Park, J., Woo, S., Lee, J.Y., Kweon, I.S.: Bam: Bottleneck attention module. arXiv preprint arXiv:1807.06514 (2018)
22. Paszke, A., Gross, S., Massa, F., Lerer, A., Bradbury, J., Chanan, G., Killeen, T., Lin, Z., Gimelshein, N., Antiga, L., Desmaison, A., Köpf, A., Yang, E., DeVito, Z., Raison, M., Tejani, A., Chilamkurthy, S., Steiner, B., Fang, L., Bai, J., Chintala, S.: Pytorch: An imperative style, high-performance deep learning library. ArXiv **abs/1912.01703** (2019)
23. Ren, S., He, K., Girshick, R., Sun, J.: Faster r-cnn: Towards real-time object detection with region proposal networks. Advances in neural information processing systems **28**, 91–99 (2015)
24. Sandler, M., Howard, A., Zhu, M., Zhmoginov, A., Chen, L.C.: Mobilenetv2: Inverted residuals and linear bottlenecks. In: Proceedings of the IEEE conference on computer vision and pattern recognition. pp. 4510–4520 (2018)
25. Simonyan, K., Zisserman, A.: Very deep convolutional networks for large-scale image recognition. arXiv preprint arXiv:1409.1556 (2014)
26. Szegedy, C., Liu, W., Jia, Y., Sermanet, P., Reed, S., Anguelov, D., Erhan, D., Vanhoucke, V., Rabinovich, A.: Going deeper with convolutions. In: Proceedings of the IEEE conference on computer vision and pattern recognition. pp. 1–9 (2015)
27. Tan, M., Le, Q.: Efficientnet: Rethinking model scaling for convolutional neural networks. In: International Conference on Machine Learning. pp. 6105–6114. PMLR (2019)
28. Vaswani, A., Shazeer, N., Parmar, N., Uszkoreit, J., Jones, L., Gomez, A.N., Kaiser, Ł., Polosukhin, I.: Attention is all you need. In: Advances in neural information processing systems. pp. 5998–6008 (2017)
29. Wang, F., Jiang, M., Qian, C., Yang, S., Li, C., Zhang, H., Wang, X., Tang, X.: Residual attention network for image classification. In: Proceedings of the IEEE conference on computer vision and pattern recognition. pp. 3156–3164 (2017)
30. Wang, Q., Wu, B., Zhu, P., Li, P., Zuo, W., Hu, Q.: Eca-net: Efficient channel attention for deep convolutional neural networks. In: 2020 IEEE/CVF Conference on Computer Vision and Pattern Recognition (CVPR). pp. 11531–11539 (2020). https://doi.org/10.1109/CVPR42600.2020.01155
31. Wang, X., Girshick, R., Gupta, A., He, K.: Non-local neural networks. In: Proceedings of the IEEE conference on computer vision and pattern recognition. pp. 7794–7803 (2018)
32. Woo, S., Park, J., Lee, J.Y., Kweon, I.S.: Cbam: Convolutional block attention module. In: Proceedings of the European conference on computer vision (ECCV). pp. 3–19 (2018)
33. Xie, S., Girshick, R., Dollár, P., Tu, Z., He, K.: Aggregated residual transformations for deep neural networks. In: Proceedings of the IEEE conference on computer vision and pattern recognition. pp. 1492–1500 (2017)
34. Xu, K., Ba, J., Kiros, R., Cho, K., Courville, A., Salakhutdinov, R., Zemel, R., Bengio, Y.: Show, attend and tell: Neural image caption generation with visual attention. Computer Science pp. 2048–2057 (2015)

35. Zagoruyko, S., Komodakis, N.: Paying more attention to attention: Improving the performance of convolutional neural networks via attention transfer. arXiv preprint arXiv:1612.03928 (2016)
36. Zhang, H., Wu, C., Zhang, Z., Zhu, Y., Lin, H., Zhang, Z., Sun, Y., He, T., Mueller, J., Manmatha, R., et al.: Resnest: Split-attention networks. arXiv preprint arXiv:2004.08955 (2020)
37. Zhang, X., Zhou, X., Lin, M., Sun, J.: Shufflenet: An extremely efficient convolutional neural network for mobile devices. In: Proceedings of the IEEE conference on computer vision and pattern recognition. pp. 6848–6856 (2018)